Ferrofluid nucleus phase transitions in an external uniform magnetic field

B. M. Tanygin†, S. I. Shulyma, V. F. Kovalenko, and M. V. Petrychuk

Faculty of Radiophysics, Taras Shevchenko National University of Kyiv, 4G, Acad. Glushkov Ave., Kyiv 03187, Ukraine

(Received 13 March 2015; revised manuscript received 5 May 2015; published online 20 September 2015)

The phase transition between a massive dense phase and a diluted superparamagnetic phase has been studied by means of a direct molecular dynamics simulation. The equilibrium structures of the ferrofluid aggregate nucleus are obtained for different values of a temperature and an external magnetic field magnitude. An approximate match of experiment and simulation has been shown for the ferrofluid phase diagram coordinates "field–temperature". The provided phase coexistence curve has an opposite trend comparing to some of known theoretical results. This contradiction has been discussed. For given experimental parameters, it has been concluded that the present results describe more precisely the transition from linear chains to a dense globes phase. The theoretical concepts which provide the opposite binodal curve dependency trend match other experimental conditions: a diluted ferrofluid, a high particle coating rate, a high temperature, and/or a less particles coupling constant value.

Keywords: ferrofluid, aggregate, phase diagram, molecular dynamics

PACS: 47.65.Cb, 02.70.Ns **DOI:** 10.1088/1674-1056/24/10/104702

1. Introduction

Ferrofluids (FF) are colloidal suspensions of magnetic nanoparticles in a carrier liquid. An increasing interest to FF is related to their applications: drug deliveries,[1] a hyperthermia,[2] a magneto-resonance tomography,[3] and so on.[4–7] Additionally, phase transitions fundamental understanding can be developed by means of FF usage as a model system.

Suspended and aggregated phases are two major possible states of an FF matter.[8,9] A vessel volume contains a single phase or multiple FF phases.[10] A more detailed systematization of dense phases is determined by an aggregates substructure classification (spatial ordering and symmetry) which impacts on thermodynamic properties. Some of possible FF aggregates are: drop-like aggregates[10–12] (either bulk drops or microdrops), one-dimensional chains,[13–16] labyrinthine patterns,[17] hexagonal patterns,[18] rod-shaped[19,20] aggregates, dumbbell-like aggregates,[20,21] etc. Phase transitions correspond to all possible pairs of these phases. Forced phase transitions can be triggered by an external magnetic field applying and/or temperature changes or through other external impact.

The phase transition between the suspended and aggregated phases has been called by a liquid–gas (LG) phase transition.[9] A contradiction between different FF LG phase transition research results exists:[9] while it is predicted by theories[10,22–26] and observed in some experiments,[27] simulation research reports (e.g. Ref. [28]) usually exclude the LG phase transition possibility or provides a phase diagram which does not match an expected one.[9] It has been concluded that mean-field and statistical models are not justified in the case of large coupling constant and/or large densities of FF nanoparticles.[29] Other aspects of the above-mentioned contradiction will be discussed in the present work.

A material memory-related phenomenon is detected experimentally for drop-like aggregates. The phase diagram evolves after a cyclic heating and cooling: temperature and field magnitude transition values depend on a sequential cycle number.[30,31] This effect as well as similar ones cannot be explained in scope of theories which imply an FF as a continuous medium of separate particles. Such thermodynamical (statistical) theories[22,24–26,32–35] require assumptions leading to an analytical closed-form expression derivation possibility. Some of these theories are phenomenological (e.g. Ref. [25]). Examples of the simplification-related assumptions of these models are following: the nearest-neighbors approximation of configurational integral,[10] the isotropic potential approximation,[36] a dipole–dipole interaction as a perturbation,[24] a very diluted phase consideration,[37,38] a zero or infinite value of an external magnetic field,[10] and so on.[39] Some of these models[36] imply the Boltzmann factor-based statistical averaging over all possible magnetic moments pair orientations. However, this model assumes a uniform statistical distribution over particles mutual positions which is justified only in the case of a high-temperature FF with a small correlation of magnetic moments orientations.[26] This assumption works in the case of a temperature close or higher than a critical temperature of an FF. Similar model shows matching an experiment in the case of a diluted enough FF: a volume fraction value of an FF dispersed phase was 2.4%.[24]

†Corresponding author. E-mail: b.m.tanygin@gmail.com

© 2015 Chinese Physical Society and IOP Publishing Ltd

This match has been shown only for a sedimentation direction of a phase transition in contrast of a "melting"[33] of a dense phase.

A short review and comparison of phase transitions investigations in theoretical, experimental, and numerical simulation research works have been reported in Ref. [10]. The idealized "homogeneous" FF models treats the phase transition as the van der Waals LG transition of an ensemble of separate particles. This assumption leads to the problems of matching of the theory and the experiment.[10] Any heterogeneous clusters (e.g. one-dimensional chains or coil-like structures) are not covered by such models. A detailed study of FF aggregates equilibrium internal structure shows a much wider variety of possible structures.[14,15] A thermodynamic stability of FF aggregate structures leads to an emergence of a gap between branches of a binodal of a coexistence of dense and dilute phases.[10]

In order to take into account a variety of possible spatial and spin configurations of a dipolar system, a numerical modeling-based research work is required. There are two major types of such methods: molecular dynamics (see e.g. Refs. [29] and [40] and references therein) and Monte Carlo (see e.g. Refs. [38] and [41] and references therein) simulations. In scope of a conventional assumption that the Brownian particles motion does not require a quantum mechanics-based description,[42] a molecular dynamics is a possible candidate to be an *ab initio* method of an FF numerical research. Another assumption is implicit solvation (continuum solvation)[43] approximation of Brownian particle motion. Most molecular dynamics simulations focus on systems with periodical boundary conditions.[29,40] A comprehensive comparison of a theory, a simulation, and an experiment has been reported for magnetization curves only.[44] Concerning phase diagrams, such comparison is either non-quantitative or requires an introduction and a variation of *ad hoc* unknown parameters leading to an expected match: magnetic core-size distribution functions (a polydispersity), a nonspherical particle shape, the Hamaker constant A_{H} precise value definition problem,[33] the van der Waals forces microscopic theory approximation including many-body interactions,[45–47] a nonmagnetic part of a nanoparticle volume, a stabilizing surfactant layer interaction nature (formula and constants),[29] a coverage rate of a nanoparticle by a surfactant, solvation layers,[24] aggregating characteristic parameter,[25] etc. There is a lack of numerical research works which match experimental phase transitions parameters[30,31,48–51] even via the selection of the abovementioned *ad hoc* parameters. According to Ref. [10], existing simulation methods[29,37,38,40,52–55] provides mostly linear chain-like aggregates. Hence, the phase transition between a massive dense phase[14] and a diluted superparamagnetic phase is not yet enough studied by a direct molecular dynamics simulation.

Our previous published simulation method had been designed to the purpose of a monodisperse FF aggregation research in the case of large magnetite particles (diameter 20 nm).[14] A smaller size of magnetite particles ($\approx$ 10 nm or less) corresponds to a predominance of the Brownian motion comparing to aggregating forces.[56,57] Hence, in real polydisperse FF complex phase transitions and phases coexistence are possible.[10,24] The subject of the present research is the phase transitions in the polydisperse FF under applied temperature and magnetic field changes. For this purpose, the original simulation method should be improved and validated by a comparison with related experimental research.[30,31]

2. Model and simulation

2.1. Particle model and interactions

If a deviation of a nanoparticle shape from a spherical one has isotropic probability distribution then one could consider particles as hard spheres.[56] The i-th particle hydrodynamical diameter $d_i = d_i^{\mathrm{m}} + 2a_0 + 2\delta$ consists of a ferromagnetic core diameter d_i^{m}, a nonmagnetic surface layer thickness which equals a lattice constant a_0 of a respective bulk crystalline material, and a stabilizing surfactant layer thickness δ.[56,57] We will consider only single-domain particles with $d_i^{\mathrm{m}} < d_0$,[58] where the single-domain particle size threshold is $d_0 < 0.5$ μm.[59–61] A stabilizing surfactant molecules surface density N_{S} on a particle determines a rate of its coating and impacts on the FF stabilization.[56]

The Rayleigh dissipation function of an N particles system includes each particle degrees of freedom ($i = \overline{1,N}$): center of mass spatial coordinates $\boldsymbol{r}_i$, Euler angles of a particle rotation, and a magnetic moment $\boldsymbol{m}_i$ where $|\boldsymbol{m}_i| = \mathrm{const}$. A particle potential energy depends on its Euler angles implicitly through an angle θ_i between $\boldsymbol{m}_i$ and a particle easy magnetization axis unit vector $\boldsymbol{n}_i$.[57]

The total force acting on the i-th nanoparticle is given by:

$$\boldsymbol{F}_i = \boldsymbol{F}_i^{\mathrm{f}} + \sum_j \left(\boldsymbol{F}_{ij}^{\mathrm{dd}} + \boldsymbol{F}_{ij}^{\mathrm{W}} + \boldsymbol{F}_{ij}^{\mathrm{ER}} + \boldsymbol{F}_{ij}^{\mathrm{HS}} \right). \tag{1}$$

Assuming the limit of low Reynolds number, the viscous friction force is given by the Stokes' law $\boldsymbol{F}_i^{\mathrm{f}} = -3\pi\eta d_i \boldsymbol{v}_i \equiv -\gamma_i^{\mathrm{T}} \boldsymbol{v}_i$ where η is a carrier liquid dynamic viscosity and $\boldsymbol{v}_i$ is the i-th particle velocity. The $\boldsymbol{F}_{ij}^{\mathrm{dd}}$ is a dipole–dipole interaction force.[14,29,57] The van der Waals' interaction energy between spherical bodies is given in Ref. [62]. Its differentiation yields the force:

$$\boldsymbol{F}_{ij}^{\mathrm{W}} = \boldsymbol{\rho}_{ij} \frac{-32 A_{\mathrm{H}} z {R_i}^3 {R_j}^3}{3\left[z^2 - (R_i - R_j)^2\right]^2 \left[z^2 - (R_j + R_i)^2\right]^2}, \tag{2}$$

where A_{H} is the Hamaker constant; a radius $R_i \equiv a_0 + d_i^{\mathrm{m}}/2$; a distance $z = |\boldsymbol{r}_i - \boldsymbol{r}_j|$; and its dimensionless value $\boldsymbol{\rho}_{ij} = (\boldsymbol{r}_i - \boldsymbol{r}_j)/z$. The energy density of entropic repulsion[63] of two surfaces:

$$E_{\mathrm{f}} = kTN_{\mathrm{S}}\left[1 - s/(2\delta)\right] \tag{3}$$

after an integration over surfaces of two particles with different radii takes the form (at $z \le R_i + R_j + 2\delta$):

$$G_{ij}^{\mathrm{ER}} = \frac{\pi kTN_{\mathrm{S}}\left[z-(2\delta+R_j+R_i)\right]^2\left[(R_j+R_i)^2(z+\delta)-(R_i^3+R_j^3)\right]}{6\delta z(R_i+R_j)}, \tag{4}$$

where k is the Boltzmann constant; T is a thermodynamic temperature; s is a distance between surfaces; δ is a surfactant molecule length. In the case of particles of the same radii, the closed-form expression equation (4) differs from the well-known logarithmic one.[63,64] However, these dependencies are numerically close to each other with the tolerance $\sim 20\%$ for particles with diameter 10 nm. Existing experimental results cannot justify these expressions difference. The comparison of the derivation procedures will be published separately.

The corresponding force $\boldsymbol{F}_{ij}^{\mathrm{ER}} = -\partial G_{ij}^{\mathrm{ER}}/\partial \boldsymbol{r}_i$ is given by

$$\begin{aligned}\boldsymbol{F}_{ij}^{\mathrm{ER}} = & -\boldsymbol{\rho}_{ij}\pi kTN_{\mathrm{S}}(z-2\delta-R_2-R_1)(R_2+R_1) \\ & \times\left\{2\left(z^2+\delta^2\right)-\left(R_2^2-R_1R_2+R_1^2\right)\left(\frac{z}{R_2+R_1}+1\right)\right. \\ & \left.+\delta z+\frac{\left[2R_1R_2-(R_1-R_2)^2\right]\delta}{R_2+R_1}\right\}\Big/(6\delta z^2).\end{aligned} \tag{5}$$

The hard-sphere model[26] force is given by the following expression:

$$\boldsymbol{F}_{ij}^{\mathrm{HS}} = \begin{cases}\infty\cdot\boldsymbol{\rho}_{ij}, & \text{at } z \le (d_i+d_j)/2, \\ \boldsymbol{0}, & \text{at } z > (d_i+d_j)/2.\end{cases} \tag{6}$$

The total effective torque acting on the i-th particle is determined by a viscous rotational friction, a particle anisotropy, the applied external magnetic field $\boldsymbol{B}_0$ value, and a dipole–dipole interaction field:[29,52,57]

$$\begin{aligned}\boldsymbol{\tau}_i = & -\gamma_i^{\mathrm{R}}\boldsymbol{\omega}_i + KV_i\sin(2\theta_i)\left[\boldsymbol{n}_i\times\boldsymbol{m}_i\right]/\sin(\theta_i) \\ & +\left[\boldsymbol{m}_i\times\left(\boldsymbol{B}_0+\sum_j\boldsymbol{B}_j\right)\right],\end{aligned} \tag{7}$$

where $\gamma_i^{\mathrm{R}} = 6V_i\eta$; $V_i = \pi(d_i^{\mathrm{m}})^3/6$ is the i-th particle magnetic core volume; K is a particle magnetic anisotropy constant; the $\boldsymbol{\omega}_i$ is the i-th particle self-rotation angular velocity; $\boldsymbol{B}_j$ is a magnetic field created by the j-th particle magnetic moment in the geometric center of the i-th particle. All types of magnetic anisotropies should be taken into account: a magnetocrystalline anisotropy,[65] a shape anisotropy (demagnetization tensor),[66] an anisotropy of surface,[67] etc.

2.2. Translational and rotational motion

In scope of the continuum solvation approximation of not very dense solutions, the Brownian translational and rotational particle motion is described by the Langevin equations with the hydrodynamic-originated Langevin parameters:[29,40,52,68,69]

$$M_i\mathrm{d}^2\boldsymbol{r}_i/\mathrm{d}t^2 = \boldsymbol{F}_i + \boldsymbol{\xi}_i^{\mathrm{T}}, \tag{8}$$

$$I_i\mathrm{d}\boldsymbol{\omega}_i/\mathrm{d}t = \boldsymbol{\tau}_i + \boldsymbol{\xi}_i^{\mathrm{R}}, \tag{9}$$

where M_i and I_i are the i-th particle mass and moment of inertia respectively; t is a time; $\boldsymbol{\xi}_i^{\mathrm{T}}$ and $\boldsymbol{\xi}_i^{\mathrm{R}}$ are random force and torque respectively, which are usually modelized by Gaussian noise:[29,40,69,70]

$$\left\langle\boldsymbol{\xi}_i^{\mathrm{T}}(t)\right\rangle = 0, \tag{10}$$

$$\left\langle\boldsymbol{\xi}_i^{\mathrm{T}}(t)\,\boldsymbol{\xi}_i^{\mathrm{T}}(t')\right\rangle = 6kT\gamma_i^{\mathrm{T}}\delta(t-t'), \tag{11}$$

$$\left\langle\boldsymbol{\xi}_i^{\mathrm{R}}(t)\right\rangle = 0, \tag{12}$$

$$\left\langle\boldsymbol{\xi}_i^{\mathrm{R}}(t)\,\boldsymbol{\xi}_i^{\mathrm{R}}(t')\right\rangle = 6kT\gamma_i^{\mathrm{R}}\delta(t-t'), \tag{13}$$

where $\delta(t)$ is the Dirac delta.

It is important to note that original Langevin equations were supplemented by particles interaction forces (1) and torques (7). This supplementation has been considered as an obvious and intuitive step which had been made in scope of the molecular dynamics simulation-based research programs.[29,40,52] However, it still should be exactly theoretically justified in general case of the Brownian particle motion. This statement is in need of further research.

A rotation of a magnetic moment inside a particle is described by the Landau–Lifshitz–Gilbert equation with the attempt time $t_0 = M_{\mathrm{s}}/2\alpha\gamma K$ where M_{s} is a saturation magnetization; α is a damping factor; γ is an electron gyromagnetic ratio.[57] The simultaneous Brownian dynamics of a magnetic moment and a particle has been investigated in Ref. [71].

2.3. Experimental and simulation parameters

All parameters of the present simulation correspond to the specific experiment.[30,31,72] The considered FF consists of the magnetite nanoparticles suspended in the kerosene carrier liquid. The stabilizing surfactant is the oleic acid ($\delta = 2$ nm [56]). The particles diameter distribution was determined experimentally.[72] The mean diameter is $\bar{d} = 11.5$ nm. The magnetite lattice parameter $a_0 \approx 0.8397$ nm corresponds to the cubic spinel structure with the space group $Fd3m$ (above the Verwey temperature).[73,74] However, this parameter is approximate because only 10% of particles have a crystal structure. This conclusion was made based on a dark field electron microscopy measurements.[72] The simulation initial condition is a random close packing[75] (cf. Ref. [33]) of particles positions and random magnetic moments directions. The

external magnetic field is uniform. Dielectric properties of the surfactant layer are generally similar to those of the carrier liquid.[33] Hence, the Hamaker constant of a magnetite is $A_{\rm H} = 4 \cdot 10^{-20}$ J.[33]

A required step of a dense phase emergence is an original phase nucleus forming. Consequently, a phase diagram of a nucleus is close to a phase diagram of a bulk FF phase. Only the nucleus aggregate will be considered in this simulation. Hence, a number of particles N should be minimal but not less some threshold where a phase diagram start significant changes depending on the N: a transition from a bulk phenomenon to a surface one. Number $N \sim 100$ has been selected for the polydisperse FF with a lognormal distribution.

The magnetic moment precession attempt (damping) time order of magnitude is $\tau_0 \sim 10^{-10}$ s–10^{-9} s.[56] In the case of particles $d_i \leq \bar{d}$, the Néel relaxation time $\tau_{\rm N}$ and the Brownian relaxation time $\tau_{\rm B}$ relates as:[56,63]

$$\tau_{\rm N} < \tau_{\rm B} \leq 10^{-6}\,({\rm s}). \tag{14}$$

Most part of the range $0 < d \leq \bar{d}$ corresponds to the relation $\tau_{\rm N} \ll \tau_0$. In this case both the Néel relaxation flip and a magnetic moment dynamics should be considered. The Brownian rotation is a much slower process. A particle rotation does not impact on a magnetic configuration and a free energy of the phase.

The relation is opposite for the larger particles $d_i > \bar{d}$:[57]

$$\tau_0 \ll 10^{-6}\,({\rm s}) < \tau_{\rm B} < \tau_{\rm N}. \tag{15}$$

Here, a magnetic moment alignment with an effective field can be modeled as instant. The magnetic moment rotates the particle through anisotropy forces. We suppose that the high enough anisotropy energy KV gradient leads to the model with the magnetic moment "frozen" into the particle. The vector $\boldsymbol{m}_i$ is followed by the vector $\boldsymbol{n}_i$:

$$\boldsymbol{m}_i \,||\, \boldsymbol{n}_i. \tag{16}$$

The saturated surface density of a number of oleic acid molecules in a particle coating is $N_{\rm S}^{\rm max} = 2 \cdot 10^{18}$ m^{-2}.[56] Depending on an FF preparation recipe variation (an order of mixing/heating of different components,[72] etc.), the coating rate $k_{\rm c} = N_{\rm S}/N_{\rm S}^{\rm max}$ can differ. A classical well-stabilized FF usually has $k_{\rm c} \sim 50\%$ which blocks the particles aggregation during durable timeframes (years) due to the free energy barrier 15 kT–25 kT (Fig. 1(a)).[56] The Brownian motion kinetic energy ~ 1 kT is not enough to overpass the barrier. Only larger particles form aggregates,[10,14] which corresponds to the potential well at the $l \approx 0.5$ (Fig. 1(a)). In the experimental research[31] the $k_{\rm c}$ value had been reduced, which leads to the dense phase (drop-like aggregates) emergence (Fig. 1(b)). Same mesoscopic organization control has been reported in Ref. [76]. The value $k_{\rm c} = 5\%$ has been selected for the present simulation. The calculation of an entropy and the corresponding free energy F by the Eyring's free volume theory[77] based algorithm[33] has been made for the system of particles used in the present simulation (Fig. 2). The potential well required for the dense phase emergence is 2 kT–4.5 kT or more.[24] An equilibrium state corresponds to the dense phase of such FF. A particles contact leads to an infinite negative potential energy of the van der Waals interaction. The entropic repulsion cannot counteract. However, particles mutual attraction is reversible due to an existence of a minimal distance between their surfaces $s_{\rm min} < \delta$ (Fig. 1(b)). The value $s_{\rm min} = 0.5\,a_0$ nm has been selected as a half of a cell constant which qualitatively reflects restrictions of the Hamaker theory-approximated consideration of spherical particles as a continuous body (2) in the case of distances comparable to atomic scale. It corresponds to surface structure peculiarities, a nanoparticle quasicrystalline structure, etc. On the other hand, the value $s_{\rm min}$ corresponds to an order of magnitude of two oleic acid molecular widths. This additional to the entropic repulsion (4) stabilized "buffer" role of the surfactant molecule has been discussed in Ref. [56].

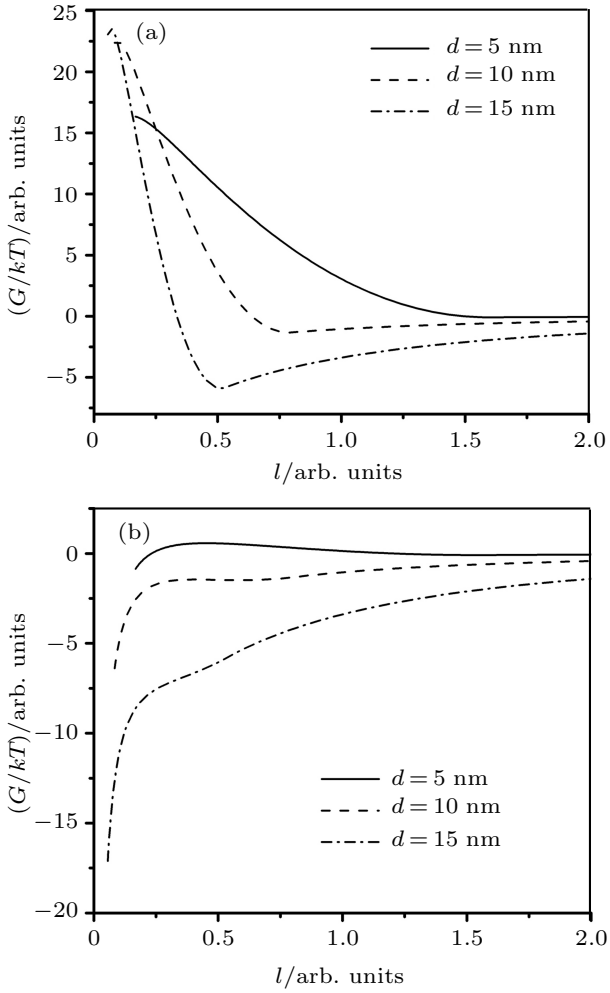


Fig. 1. Potential energy dependence on the dimensionless distance between two identical magnetite particles surfaces $l = 2s/d$. Different particles diameters d are specified. (a) Coating rate by the oleic acid: $k_{\rm c} = 50\%$ and (b) coating rate by the oleic acid: $k_{\rm c} = 5\%$.

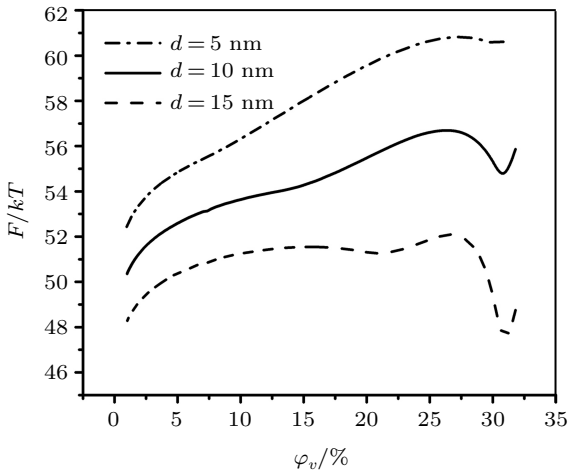


Fig. 2. Average free energy of the particle in the aggregate with 100 particles with random positions which fits to the density. The dependence on the volume fraction of the ferrofluid dispersed phase is shown. Coating rate by the oleic acid is $k_c = 5\%$. Different particles d diameters are specified.

2.4. Finite-difference scheme

The finite-difference Euler scheme is based on the original method.[14] The only changes will be described below. Algorithm details of the present method can be accessed and contributed in the open-source project "Ferrofluid Aggregates Nano Simulator".[78] The Verlet type of a finite-difference method[79] is in need of further method improvement.

A random particle translation and rotation is considered by means of the viscous limit approximation[57,69,80] which restricts a time tolerance corresponding to a finite-difference scheme time step:

$$\Delta t \gg \max_i \left(\tau_v^{\mathrm{T}}, \tau_v^{\mathrm{R}}\right), \tag{17}$$

where $\tau_v^{\mathrm{T}} = M_i/\gamma_i^{\mathrm{T}}$ and $\tau_v^{\mathrm{R}} = I_i/\gamma_i^{\mathrm{R}}$. Consequently, an inertial term of the motion equations (8) and (9) can be neglected.[69] After the integration by the technique[69] taking into account Eqs. (10)–(13) one can obtain particle random motion dispersions $\sigma_i^{\mathrm{T}} \equiv \langle(\Delta \boldsymbol{r}_i)^2\rangle$ and $\sigma_i^{\mathrm{R}} \equiv \langle(\Delta \boldsymbol{\varphi}_i)^2\rangle$ respectively (cf. Ref. [29]):

$$\begin{aligned}\sigma_i^{\mathrm{T}} &= D_i^{\mathrm{T}}\left\{6\Delta t + (M_i/\gamma_i^{\mathrm{T}})\left[-3 + 4\exp(-\gamma_i^{\mathrm{T}}\Delta t/M_i)\right.\right. \\ &\quad \left.\left. - \exp(-2\gamma_i^{\mathrm{T}}\Delta t/M_i)\right]\right\} \qquad (18)\\ \sigma_i^{\mathrm{R}} &= D_i^{\mathrm{R}}\left\{6\Delta t + (I_i/\gamma_i^{\mathrm{R}})\left[-3 + 4\exp(-\gamma_i^{\mathrm{R}}\Delta t/I_i)\right.\right. \\ &\quad \left.\left. - \exp(-2\gamma_i^{\mathrm{R}}\Delta t/I_i)\right]\right\}, \qquad (19)\end{aligned}$$

where vector $\Delta\boldsymbol{\varphi}_i$ defines the i-th particle rotation (an axis-angle representation; $\mathrm{d}\boldsymbol{\varphi}_i/\mathrm{d}t \equiv \boldsymbol{\omega}_i$); diffusion coefficients are given by the Stokes–Einstein translational and rotational equations: $D_i^{\mathrm{T}} = kT/\gamma_i^{\mathrm{T}}$ and $D_i^{\mathrm{R}} = kT/\gamma_i^{\mathrm{R}}$ respectively. The corresponding normal distribution (Wiener process of Brownian motion) of $\boldsymbol{\xi}_i^{\mathrm{T}}$ and $\boldsymbol{\xi}_i^{\mathrm{R}}$ is calculated by the Mersenne twister algorithm.[81]

The magnetic moment Néel (14) and Brownian (15) relaxation types correspond to different calculation algorithms of the magnetic moment motion which were distinguished by a particle diameter criterion. In the case of the Néel type and $\Delta t \gg \tau_{\mathrm{N}}$, the magnetic moment was aligned with the total magnetic field direction in the i-th particle center $\boldsymbol{r}_i$ at each simulation step. In the case of the Brownian type, the rotational motion (9) of the particle with the "frozen" (16) magnetic moment is calculated.

3. Results and discussion

3.1. Equilibration state calculation

An evolution of the initial random close packing structure (Fig. 3) to the thermodynamically equilibrium state was calculated. In the case of the dense phase (the nucleus equilibration at the end of the simulation), after a stabilization period $t_{\mathrm{s}} = t_{\mathrm{s}}(H_0, T)$, a total moment of inertia of the system I_{tot} is not changing except its random fluctuations (Fig. 4). This statement has been validated up to $t = 0.2$ s for all obtained dense phases. The resulted structures are shown in Figs. 5 and 6. In order to distinguish a diluted and dense phase, simpler and similar approach comparing to a conventional correlation function is used. A one-dimensional chain[13–16] is defined in the present simulation as a cluster of particles which satisfies the condition $\left|\boldsymbol{\rho}_{i(i+1)}\right| \leq d_i + d_{i+1}$ where the i-th and $(i+1)$-th particles are neighbors in the chain. Here, each particle can have only 1 or 2 neighbors. A circle is a particular case of such a chain. A set of separated arbitrary length one-dimensional chains is being considered as a diluted phase. If stabilized equilibrium state (see Fig. 4) corresponds to at least single particle with the number of neighbors larger than 2 then the more complex dense structure is formed. This phase is defined as a dense phase by definition.

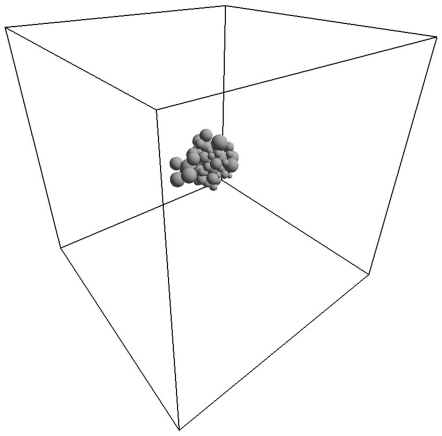


Fig. 3. Initial conditions: perspective projection. A space is limited by the cubic vessel with the edge length $L = 0.3$ μm.

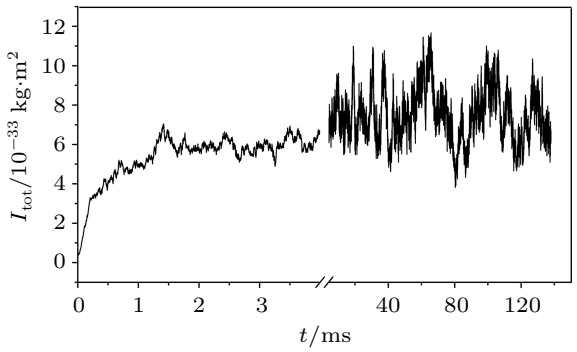


Fig. 4. Total moment of inertia time dependence at the conditions: the temperature $T = 25$ °C and the external field $H_0 = 0$ Oe (1 Oe = 79.5775 A·m^{-1}). The obtained approximated value of the dense phase stabilization period is $t_s \sim 5$ ms.

3.2. Phase diagram

The phase diagram is obtained based on an analysis of the resulted structures (Figs. 5 and 6) using a bisection method for the definition of the phase transition temperature T_t. The binodal curve of the phase diagram (Fig. 7) corresponds to the experimental results in terms of the trend and the T_t approximate value in the case of a comparison of temperature values in Kelvins.[30,31] This trend has been observed experimentally only starting from the second cycle of the system heating/cooling. The first heating corresponds to the trend weaker than experimental errors and noises.[30,31] It can be explained by the assumption that the initial experimental sample state does not correspond to the initial conditions of the simulation, i.e., the aggregate with the random close packing[75] of a polydisperse set of particles (Fig. 3). Indeed, a final equilibrium state of a non-stabilized FF is a set of primary aggregates which consist of large particles only (diameter $d_i^m \sim$ 15 nm–20 nm).[14] Hence, the first heating is required in order to produce the metastable random close packing structure which is kept within several heating/cooling cycles. The large FF aggregate transforms to the primary aggregates state after durable timeframes which require the first heating/cooling cycle again.

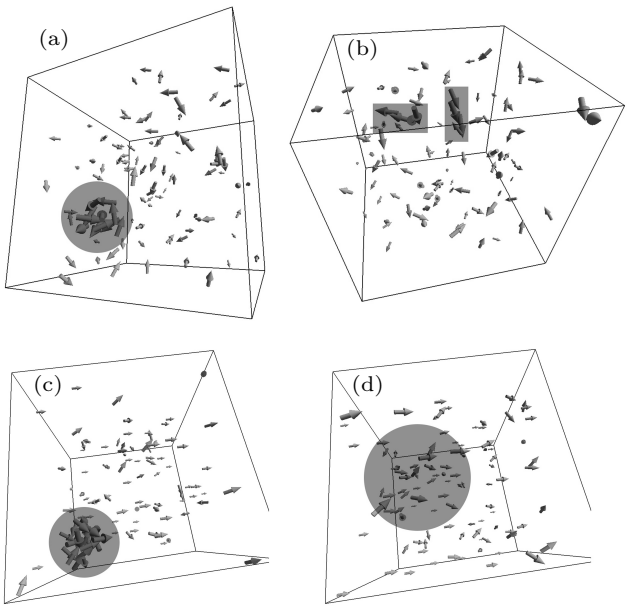


Fig. 5. Resulted thermodynamically equilibrium structures: perspective projections (area with largest particles is highlighted); $L = 0.3$ μm. A size of volumetric arrows is proportional to a geometrical size of the corresponding nanoparticle for an illustrative purpose only. (a) $H_0 = 0$ Oe and $T = 50$ °C, (b) $H_0 = 0$ Oe and $T = 75$ °C, (c) $H_0 = 200$ Oe and $T = 35$ °C, (d) $H_0 = 200$ Oe and $T = 55$ °C,

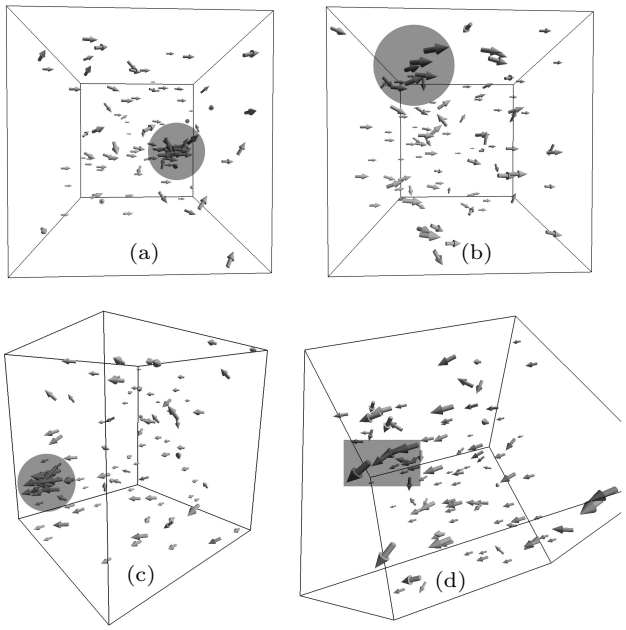


Fig. 6. Resulted thermodynamically equilibrium structures (continue). (a) $H_0 = 400$ Oe and $T = 15$ °C, (b) $H_0 = 400$ Oe and $T = 20$ °C, (c) $H_0 = 800$ Oe and $T = 0$ °C, (d) $H_0 = 800$ Oe and $T = 10$ °C,

The descending binodal curve (Fig. 7) contradicts to some theoretical investigations where this dependence is ascending.[10,24,25] As it is stated at the beginning, a contradiction between these theory conclusions and simulation reports is deeper: even a conceptual possibility of an FF LG transition emergence is being discussed among different research programs.[9] Mean-field and statistical models are not justified in the case of a large coupling constant and/or large concentration of FF nanoparticles.[29] Oppositely, they are justified in the case of a high-temperature and/or a diluted phase FF where a correlation in orientations of magnetic moments is small.[26] The latter case corresponds to a modeling of an FF by the classical Lennard-Jones (LJ) fluid and short-range order,[26,82] which excludes the possibility of an emergence of particles complex long-range ordered structures such as linear chains, rings, tubes, etc.[14,15] However, it is well established[9] that an equilibrium FF phase microstructure consists of a distribution of chains, rings or more complex structures of different lengths. Hence, a real FF dense phase should be modeled by a liquid crystal-like microstructure rather than by the classical

LJ fluid. However, the LJ fluid is a suitable model for conditions which break the long-range ordered structures through an entropy increase and a predominance of the Brownian motion: a high temperature, a low particles concentration (leading to a structures "evaporation"), a major particle coating, etc. In this case a potential energy summand of an FF free energy[33] is suppressed by an entropic summand; the free energy local minimum takes place only for large particles (the $\varphi_V < 25\%$–30% area in Fig. 2). This is why an LG transition in the framework of the LJ ferrofluid model is possible only in bi-disperse[24] or polydisperse FF thermodynamic theories.

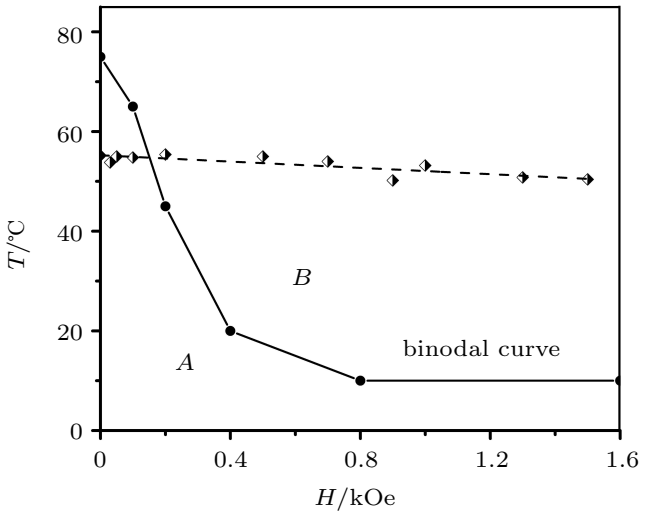


Fig. 7. Ferrofluid nucleus phase diagram: region "*A*": the aggregated phase and the diluted phase coexistence in the vessel volume; region "*B*": the diluted superparamagnetic phase only. The simulation results (circles) form a binodal curve. The experimental results[31] (diamonds) are given for a comparison.

The LJ-like ferrofluid theories correspond to the following idealizations: the continuous isotropic phase gaslike compression model;[25] a considering of a dipole–dipole interaction in scope of the perturbation theory;[24] the mean isotropic potential approximation.[10,26,36] An external magnetic field suppresses the rotational Brownian motion and aligns nanoparticles magnetic moments, which leads to a mean attraction force increase.[36] Hence, an external magnetic field stimulates the condensation phase transition[10] leading to the ascending binodal curve. In the case of a significant correlation of magnetic moments orientations (non-LJ fluid model as discussed above), this conclusion is incorrect because the mean isotropic potential model conditions have been violated: the significantly anisotropic dipole–dipole interaction strongly impacts an equilibrium structure. Such structures with a closed magnetic flux (coils, rings, ring assemblies, tubes, scrolls, etc.[15]) already correspond to a minimal potential energy and a suppressed entropic summand. The applying of an external magnetic field can only increase the potential energy: flux-closed magnetic structures (Fig. 5(a)) transform into the set of parallel linear chains (Figs. 5(c), 6(a), and 6(c)) where at least marginal particles have a less "workfunction" comparing to particles inside the ring or tube structure because they are attached to the single magnetic dipole only. Structures with a closed magnetic flux are bounded by the larger dipole–dipole energy. Such aggregate destructs at a higher temperature.

The present simulation results provide a fine structure[14,15] of the transition from "linear chains" to "dense globes" (Figs. 5 and 6) through the ring assembly structure.[14,15] Oppositely, the above-mentioned assumptions of the theoretical investigations[10,24,25] suppress this fine structure. The simulation method suggested here does not imply idealizations of the theoretical models.

The last problem which requires discussion is a relation of the opposite results to experimental studies. Both types of binodal dependencies match the respective experimental observations. Hence, their FF parameters were obviously different. The discussed contradiction has been shown only for the FF parameters of the present research:[30,31] a small particle coating rate $k_c = 5\%$ by an oleic acid which is a concept similar to Ref. [76]. This value allows a random compact packing Ref. [75] in a polydisperse FF by passing a strong surfactant repulsion. This is a non-stabilized type of an FF (Fig. 1(b)) with a high volume fraction of a dispersed phase: an equilibrium state corresponds to the value $\varphi_V \sim 30\%$. Oppositely, a "classical" stabilized FF ($k_c = 50\%$) corresponds to well-separated particles (Fig. 1(a)). The latter means that a correlation in orientations of magnetic moments is small[26] due to a larger average distance between particles and a corresponding weaker dipole–dipole interaction. In this case the aggregates formation can be modeled by an LG type of a phase transition in the framework of the simple mean-field theory[22] or the isotropic potential model.[26,36] In the case of a stabilized FF, an ascending binodal curve theoretical dependence[10,24,25] matches very few experimental reports (the reference in Ref. [24]).

This research focuses on the FF aggregate nucleus only. The phase diagram should be verified and generalized to the case of a bulk phase: a larger number of particles and a more durable period of a stabilization. According to the experiment,[30,31] this period should have order of magnitude in a range between seconds and minutes time-scales. Taking into account an extensive nature of the current simulation method,[78] its natural further development is a parallel computing capabilities implementation. In our opinion, a most promising method of the parallel computation of the

FF molecular dynamics is a Graphics Processing Units-based approach.[52] The open-source project dedicated to a further evolution of the method has been started.[78] A comparison of present results with ones based on the Monte Carlo simulation is in need of further investigations.[38,41]

4. Conclusions

(i) The equilibrium structures of the ferrofluid aggregate nucleus have been determined for different values of temperature and external magnetic field magnitude.

(ii) The simulation of the ferrofluid phase diagram, which approximately matches the experiment, is obtained.

(iii) The obtained binodal curve has an opposite (descending) trend comparing to some of known theoretical results.

(iv) In our opinion, the applied simulation method provides a more justified description of the magnetite ferrofluid with the minor rate of the particle coating by surfactant molecules.

(v) The theoretical concepts which provide the ascending binodal curve dependency trend match other experimental conditions: a diluted ferrofluid, a high particle coating rate, a high temperature, and/or a less particles coupling constant value.

Acknowledgment

We thank Mrs. Daria T for support with the graphical design of the "FFANS" web page.

References

[1] Lübbe A S, Bergemann C, Huhnt W, Fricke T, Riess H, Brock J W and Huhn D 1996 *Cancer Research* **56** 4694
[2] Jordan A, Scholz R, Wust P and Fähling H 1999 *J. Magn. Magn. Mater.* **201** 413
[3] Kim D K, Zhang Y, Kehr J, Klason T, Bjelke B and Muhammed M 2001 *J. Magn. Magn. Mater.* **225** 256
[4] Shimada K, Shuchi S, Kanno H, Wu Y and Kamiyama S 2005 *J. Magn. Magn. Mater.* **289** 9
[5] Yellen B, Friedman G and Barbee K 2004 *IEEE Trans. Magn.* **40** 2994
[6] Li X Q, Zheng L and Wang X F 2014 *Chin. Phys. Lett.* **31** 024701
[7] Yu G J, Pu S L, Wang X and Ji H Z 2012 *Acta Phys. Sin.* **61** 194703 (in Chinese)
[8] Blum Y, Mayorov M and Tsebers A 1986 *Magnitnye Zhudkosti* (Riga: Zinatne in Russian)
[9] Holm C and Weis J 2005 *Current Opinion in Colloid & Interface Science* **10** 133
[10] Zubarev A Y and Iskakova L Y 2004 *Physica A: Statistical Mechanics and its Applications* **335** 325
[11] Bacri J C, Salin D and Massart R 1982 *Journal de Physique Lettres* **43** 179
[12] Zubarev A Y and Iskakova L Y 2003 *Phys. Rev. E* **68** 061203
[13] Iskakova L Y, Romanchuk A P and Zubarev A Y 2006 *Physica A: Statistical Mechanics and its Applications* **366** 18
[14] Tanygin B, Kovalenko V, Petrychuk M and Dzyan S 2012 *J. Magn. Magn. Mater.* **324** 4006
[15] Yoon M and Tománek D 2010 *J. Phys: Condens. Matter* **22** 455105
[16] Gorenstein M I and Greiner W 2014 *Mod. Phys. Lett. B* **28** 1450039
[17] Rosensweig R E, Zahn M and Shumovich R 1983 *J. Magn. Magn. Mater.* **39** 127
[18] Richardi J and Pileni M 2004 *Phys. Rev. E* **69** 016304
[19] Moldovan B N, Antonyuk O A, Petrychuk M V and Kovalenko V F 2006 *Journal of Colloid and Interface Science* **296** 577
[20] Kovalenko V F, Petrychuk M, Moldovan N, Antonyuk A and Tkach F 2006 *Funct. Mater.* **13** 640
[21] Tanygin B M, Shulyma S I, Kovalenko V F, Petrychuk M V and Tanygina D M 2013 "Long-range Ordering of Ferrouid Aggregates and its Antiviral Applications", *Schedule and Abstracts of 3rd Frontiers in BioMagnetic Particles Meeting* (Telluride CO USA: Frontiers in BioMagnetic Particles) p. 59
[22] Sano K and Doi M 1983 *J. Phys. Soc. Jpn.* **52** 2810
[23] Yu Zubarev A and Iskakova L 2005 *Physica A: Statistical Mechanics and its Applications* **349** 1
[24] Ivanov A O 1996 *J. Magn. Magn. Mater.* **154** 66
[25] Li J, Huang Y, Liu X, Lin Y, Bai L and Li Q 2007 *Sci. Technol. Adv. Mater.* **8** 448
[26] Kalikmanov V I 1992 *Physica A: Statistical Mechanics and its Applications* **183** 25
[27] Cousin F, Dubois E and Cabuil V 2003 *Phys. Rev. E* **68** 021405
[28] Weis J and Levesque D 1993 *Phys. Rev. Lett.* **71** 2729
[29] Wang Z, Holm C and Müller H 2002 *Phys. Rev. E* **66** 021405
[30] Kovalenko V F, Petrychuk M V, Tanygin B M and Shulyma S I 2013 *Bulletin of Taras Shevchenko National University of Kyiv, Series Physics & Mathematics* 4
[31] Kovalenko V F, Petrychuk M V, Tanygin B M and Shulyma S I 2014 http://arxiv.org/abs/1404.5541 (preprint 1404.5541)
[32] Tsebers A O 1982 *Magnetohydrodynamics* **18** 345
[33] Scholten P 1983 *J. Magn. Magn. Mater.* **39** 99
[34] Cbers A 1990 *J. Magn. Magn. Mater.* **85** 20
[35] Buyevich Y and Ivanov A 1992 *Physica A: Statistical Mechanics and its Applications* **190** 276
[36] Chan D Y and Henderson D 1984 *Journal of Colloid and Interface Science* **101** 419
[37] Stevens M and Grest G 1994 *Phys. Rev. Lett.* **72** 3686
[38] Satoh A, Chantrell R W, Kamiyama S I and Coverdale G N 1996 *Journal of Colloid and Interface Science* **181** 422
[39] Mansoori G A 1971 *J. Chem. Phys.* **54** 1523
[40] Wang Z and Holm C 2003 *Phys. Rev. E* **68** 041401
[41] Camp P and Patey G 2000 *Phys. Rev. E* **62** 5403
[42] Hakim V and Ambegaokar V 1985 *Phys. Rev. A* **32** 423
[43] Ferrara P, Apostolakis J and Caflisch A 2002 *Proteins* **46** 24
[44] Ivanov A, Kantorovich S, Reznikov E, Holm C, Pshenichnikov A, Lebedev A, Chremos A and Camp P 2007 *Phys. Rev. E* **75** 061405
[45] Derjaguin B 1934 *Kolloid-Zeitschrift* **69** 155
[46] Lifshitz E M 1956 *Sov. Phys. JETP* **2** 73
[47] Langbein D 1970 *Phys. Rev. B* **2** 3371
[48] Ke Y H, Yang S Y, Horng H E, Hong C Y and Yang H C 2004 *Eur. Phys. J. B* **41** 319
[49] Morozov K, Pshenichnikov A, Raikher Y and Shliomis M 1987 *J. Magn. Magn. Mater.* **65** 269
[50] Bacri J C, Perzynski R, Cabuil V and Massart R 1989 *Journal of Colloid and Interface Science* **132** 43
[51] Bacri J C, Perzynski R, Salin D, Cabuil V and Massart R 1990 *J. Magn. Magn. Mater.* **85** 27
[52] Polyakov A, Lyutyy T, Denisov S, Reva V and Hänggi P 2013 *Comput. Phys. Commun.* **184** 1483
[53] Caillol J M 1993 *J. Chem. Phys.* **98** 9835
[54] Van Leeuwen M E and Smit B 1993 *Phys. Rev. Lett.* **71** 3991
[55] Levesque D and Weis J J 1994 *Phys. Rev. E* **49** 5131
[56] Fertman V E 1990 *Magnetic fluid guidebook*: *properties and application* (CRC Press)
[57] Shliomis M I 1974 *Soviet Physics Uspekhi* **17** 153
[58] BrownWF 1968 *J. Appl. Phys.* **39** 993
[59] Dunlop D J 1972 *Science* (New York, N.Y.) **176** 41
[60] Dunlop D J 1973 *J. Geophys. Res.* **78** 1780
[61] Butler R F and Banerjee S K 1975 *J. Geophys. Res.* **80** 4049
[62] Hamaker H C 1937 *Physica* **4** 1058
[63] Rosensweig R E 1997 *Ferrohydrodynamics* (Courier Dover Publications)

[64] Rosensweig R E, Nestor J W and Timmins R S 1965 "Ferrohydrodynamic fluids for direct conversion of heat energy", AICHE, *Industrial Chemical Engineering Symposium Series* 5 pp. 104–118
[65] Brown W F 1963 *Micromagnetics* 18 (New York: Interscience Publishers)
[66] Tandon S, Beleggia M, Zhu Y and De Graef M 2004 *J. Magn. Magn. Mater.* **271** 27
[67] Aharoni A 1987 *J. Appl. Phys.* **61** 3302
[68] Schlick T 2010 *Molecular Modeling and Simulation: An Interdisciplinary Guide* Vol. 21 (Berlin: Springer)
[69] Pottier N 2014 *Nonequilibrium Statistical Physics: Linear Irreversible Processes* (Oxford: Oxford University Press) ISBN 0198712278
[70] Mazur P and Bedeaux D 1991 *Biophys. Chem.* **41** 41
[71] Cebers A 1975 *Magnitnaya Gidrodinamika* (in Russian) **1** 79
[72] V V Padalka 2004 "Interaction of colloidal magnetic particles with magnetic and electric fields" Ph. D. Dissertation (North Caucasian State Technical University, Stavropol) (in Russion)
[73] Fleet M E 1981 *Acta Crystallographica Section B Structural Crystallography and Crystal Chemistry* **37** 917
[74] El Ghandoor H, Zidan H M, Khalil M M H and Ismail M I M 2012 *Int. J. Electrochem. Sci.* **7** 5734
[75] Song C,Wang P and Makse H A 2008 *Nature* **453** 629
[76] Lalatonne Y, Motte L, Richardi J and Pileni M P 2005 *Phys. Rev. E* **71** 011404
[77] Hildebrand J H and Scott R L 1964 *Reinhold, New York* 411
[78] Tanygin B 2015 "*Ferrofluid Aggregates Nano Simulator*" URL https://github.com/psci2195/ffans/
[79] Verlet L 1967 *Phys. Rev.* **159** 98
[80] Einstein A 1905 *Annalen der Physik* **17** 16
[81] Matsumoto M and Nishimura T 1998 *ACM Transactions on Modeling and Computer Simulation* **8** 3
[82] Fisher I Z 1964 *Statistical Theory of Liquids* (Chicago: University of Chicago Press)